Developing a Robust 3-D Characterization-Representation Framework for Modeling Polycrystalline Materials

Michael Groeber, Somnath Ghosh, Michael D. Uchic, and Dennis M. Dimiduk

This paper introduces a methodology for generating virtual grain-level microstructural volumes for computational modeling and simulation. The methodology, which allows for the incorporation of higher-fidelity descriptions of microstructures depends upon robust three-dimensional data collection, detailed microstructural quantification, and virtual microstructure generation using microstructural-based constraints.

INTRODUCTION

The direct correlation between microstructure and material properties is a basic tenet of materials science, and with the continued improvement in modern computing capabilities, the ability to include local microstructural features in simulations of microstructure evolution or mechanical response is an active area of research.[1–3] However, there has been a general disconnect between the ability to characterize microstructure and efforts to represent this information in simulations. For example, many grain structures have been shown to have non-uniform distributions of size and shape, and some also exhibit large variations in morphology and crystallography.[4] Many of these heterogeneities cannot be expressed when grain morphology is represented by a uniform array of basic shapes like spheres, cubes, or simple polyhedrons to fill space, as is typically done in many studies.[5–7]

This paper introduces a methodology for the generation of virtual grain-level microstructural volumes for computational modeling and simulation efforts, which allows for the incorporation of higher-fidelity descriptions of microstructures. The integral components of this framework are procedures for robust three-dimensional (3-D) data collection, detailed microstructural quantification, and virtual microstructure generation using microstructural-based constraints. In this article, the importance and specific role of each of these components will be discussed with respect to the problem of representing the grain structure of a nickel-based superalloy, IN100.

DATA COLLECTION AND PROCESSING

The desire to view and characterize microstructures in 3-D is not a new idea, although the tools and techniques to make this a practical reality have improved significantly in the past few years. Serial-sectioning methods,[8–12] x-ray-based techniques,[13–15] and grain separation methods[16] have all been employed to understand the 3-D structure of grains. More recently, there has been a rapid maturation of a number of instruments that can be employed to investigate microstructure in 3-D. Some of these tools include the 3-D atom probe (3DAP),[17] the dual-beam focused ion beam-scanning electron microscope (DB FIB-SEM),[18–21] synchrotron facilities,[14] and the Robo-Met.3D mechanical polisher.[22] Similar to other characterization studies, the scale of the microstructural feature of interest, the type of data required, and local availability of the instrumentation are used to define the experimental approach for data collection.

In this work, the DB FIB-SEM was chosen to serial section an IN100 superalloy sample, as the scale of the IN100 grain structure is appropriate for FIB-based experiments. A brief introduction to serial sectioning with the DB FIB-SEM will be offered here and further details can be found in previous works.[18–21] The serial sectioning experiment consisted of the repeated removal of a thin layer of material from the volume of interest using the focused ion beam. Between sections, the sample was repositioned to place the newly exposed surface in position for electron backscatter diffraction (EBSD) pattern collection. After collection of an EBSD map, the sample was returned to the previous sectioning position and the process was repeated.

A significant advantage of using the DB FIB-SEM for this experiment included the ability to automate the data collection process using built-in microscope scripting and image recognition software. Specifically, the image recognition software enabled the DB FIB-SEM to position and mill the sample with accuracy better than 50 nm, allowing for high-resolution sectioning through the micrometer-sized grains. In the experiment shown here, the sectioning thickness was set to 250 nm (0.25 μm) to limit the overall data collection times, and an EBSD map was collected for each section. These maps provide quantitative data essential for crystallographic description of the microstructure as well as automated feature segmentation, which will be discussed later.

The data presented here consisted of 184 EBSD maps and was collected over the period of three days. Note that one disadvantage of the DB FIB-SEM is the finite volume that can be interrogated (~100 μm × 35 μm × 45 μm for this multi-day experiment). However, the relatively fine scale of the IN100 microstructure yielded thousands of grains in

the volume investigated, which can be seen in Figure 1.

Following collection of the series of two-dimensional (2-D) EBSD maps, the individual sections were reconstructed into a 3-D volume by combining the entire series of maps into a single data structure. The voxel of the 3-D data volume has dimensions equal to the in-plane spacing of the data points in each EBSD map (x and y) and the sectioning thickness (z). Once the volume was constructed, the grain structure was identified using the quantitative EBSD data. The EBSD data is composed of a set of three Euler angles (φ_1,Φ,φ_2) associated with each voxel that defines its crystallographic orientation. Software codes were developed to automatically segment the grain structure from the 3-D data by grouping contiguous voxels that had the same crystallographic orientation (within a small tolerance).[23–25] Various alignment, clean-up, and filtering routines are also applied and these routines are discussed in References 23–25.

The volume produced by the reconstruction, identification, and processing routines is shown in Figure 1. In this figure, each grain is shaded based on its crystallographic orientation (similar to an inverse pole figure map). The output from this data collection and processing module is a 3-D volume where every voxel is assigned to a specific grain. Note that the reconstruction, identification, and processing routines require as input a series of EBSD maps, and there are other experimental methodologies that could be substituted for the FIB-SEM data collectio. These include mechanical polishing combined with EBSD data collection.

MICROSTRUCTURE QUANTIFICATION

The segmented voxelized volume allows for the direct measurement of microstructural parameters in 3-D, which obviates the need for stereology based methods and provides a more complete description of selected parameters such as the true size and shape of grains and the number of grain neighbors. In addition, because all parameters are measured for each individual grain, correlations between parameters can be developed. For the IN100 volume shown previously, the grain volume, number of contiguous neighbor grains, grain shape, and spatial orientation have been measured to characterize the grain morphology. Additionally, the orientation distribution function (ODF), misorientation distribution function (MoDF), and micro-texture function (MTF) have each been calculated to describe the crystallography.

The distributions of the morphological parameters are shown in Figure 2. The volume of each grain is simply calculated from the number of voxels in the grain and the known voxel volume. In Figure 2a, the grain volumes are normalized by the average grain volume, which was calculated to be 37.32 μm^3. The number of neighboring grains is computed by determining all of the grains that have voxels that neighbor the voxels in the reference grain, and this probability distribution is shown in Figure 2b. Note that the average number of neighbors was calculated to be 12.9. Grain shape is represented by the two aspect ratios, b/a and c/a, where a, b, and c represent the principal axis of a best-fit ellipsoid. This best-fit ellipsoid is determined by calculating the grain's principal moments and generating an ellipsoid with the same principal moments; this process is described in more detail in References 25 and 26. The distribution of grain shape is shown in Figure 2c, where the upper right corner corresponds to an equiaxed grain and the lower right and lower left corners correspond to a plate-like and needle-like grain, respectively.

The crystallographic parameters are shown in Figure 3. The pole figures in Figure 3a show the macroscopic texture, and the MoDF shown in Figure 3b quantifies the difference in orientations of neighboring grains. Finally, the MTF is measured by calculating the fraction of each grain's neighbors that have low misorientation (<15°). The MTF gives some information on the spatial arrangement of the low angle misorientations. It is clear from each of the plots in Figure 3 that there is no significant texture in the material. The pole figures show nearly random macroscopic texture and there are few low-angle misorientations seen in the MoDF. The MTF, while redundant in this work, can be very useful in quantifying the amount of local texture, as seen in Reference 27.

The final objective of the statistical analysis is quantifying relationships between multiple microstructural parameters. As an example, for this work, grain volume was chosen as a free parameter and all other parameters were considered as functions of volume. First, the volume distribution was partitioned into bins by converting each grain volume into an equivalent sphere diameter and each grain was placed in a bin correlating with its diameter, as outlined in Reference 25. Then, the distribution of every other morphological parameter was calculated with respect to diameter. Figure 4 shows two examples of these correlations for the number of neighbors versus grain size and neighbor grain size versus grain size. In Figure 4 one can observe that the number of neighboring grains has a strong relationship with grain size, but the sizes of the neighboring grains are relatively independent of the reference grain's size.

MICROSTRUCTURE REPRESENTATION FOR COMPUTATIONAL MODELING

Beyond statistical characterization of 3-D microstructures, there is an additional need to supply modeling and simulation efforts with realistic grain-level microstructures. For example, experimentally collected 3-D voxel data could be directly meshed for finite element (FE) analysis, or the voxelized data could be smoothed to help remove aliasing and then meshed for FE analysis. While direct conversion of the experimental data into a form suitable for modeling and simulation provides an extremely realistic input, one limitation with this approach is that a new data set needs to be collected each time one requires a different microstructural arrangement. The data collection process is somewhat time consuming and thus, limited in scale. Therefore, in addition to developing direct conversion processes, as done by the authors in References 23 and 24, a new methodology has been developed for creating synthetic microstructures that are statistically equivalent to the experimental microstructure. These synthetic forms can supply modeling and simulation efforts with an endless supply of statistically equivalent microstructure representations and can have various levels of complexity depending on the requirements of the model input. Tes-

sellation and growth models have been previously used by a number of researchers to create synthetic microstructures.[5,28] However, the statistical inputs used in these efforts have often been generated from a 2-D analysis. The 3-D characterization discussed previously allows for more accurate and potentially more sophisticated descriptors to constrain the synthetic microstructure generation process. A custom suite of programs has been developed in this work to generate statistically equivalent synthetic microstructures.

The first module, Equivalent Ellipsoidal Grain Generator (EEGG), generates a list of grains to be placed within the model volume. The inputs required for this module are the volume cumulative probability density function (CPDF), the CPDFs of aspect ratios b/a and c/a as a function of grain volume, and the spatial orientations of the experimental grains. The EEGG samples the volume CPDF and after generating a volume, EEGG samples the b/a and c/a CPDF for the given volume. The combination of volume and two aspect ratios fully defines the ellipsoid that represents the grain. Finally, the spatial orientation of the grain is assigned. The orientation of the principal axes relative to the global axes is described by a set of three angles (λ,θ,ψ). The process of spatial orientation assignment is analogous to the crystallographic orientation assignment presented in Reference 29 and also used later in this work.

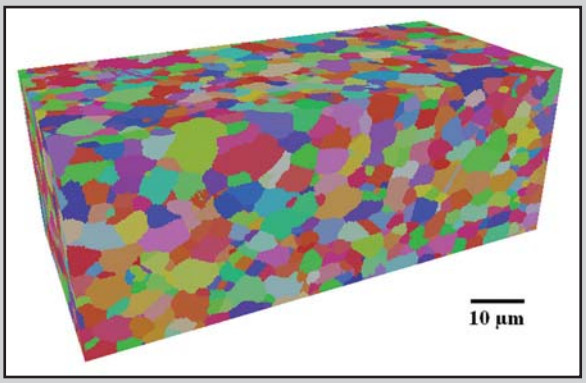

Figure 1. The microstructure of IN100 nickel-based superalloy. The volume shown here has dimensions of 96.5 µm × 36 µm × 46 µm. There are approximately 4,400 grains in the volume (after twins were artificially removed from the structure).

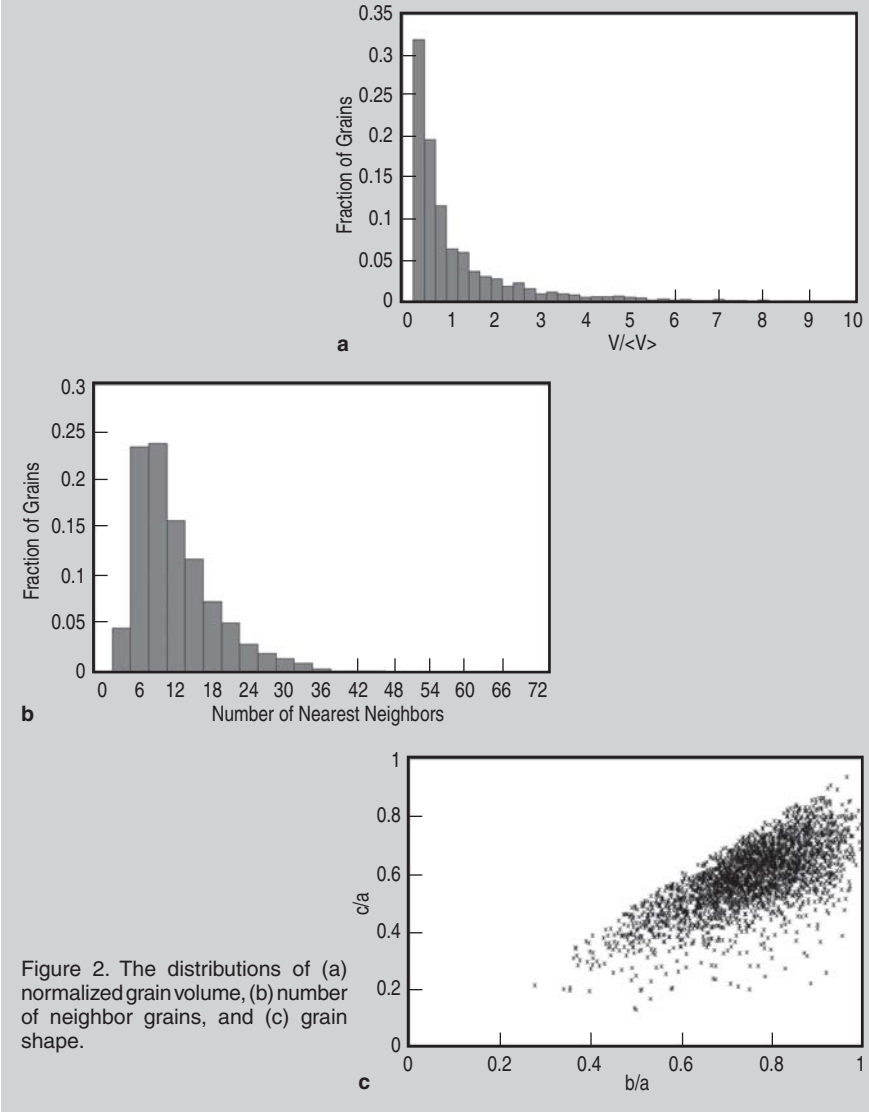

Figure 2. The distributions of (a) normalized grain volume, (b) number of neighbor grains, and (c) grain shape.

The second module, Constrained Grain Packer (CGP), focuses on the arrangement of the grains inside the model volume and as an output provides a voxelized 3-D data structure. The statistical relationships used in this process are the number of neighboring grains as a function of grain volume and the distribution of neighboring grain sizes as a function of grain volume. The grains generated by the EEGG are sequentially placed within the model volume, but before a grain can be successfully placed, multiple criteria must be met to ensure the suitability of the potential location. For example, one criterion involves the number of neighbors of the grains placed prior to the current grain. The addition of the new grains increases the number of neighbors of the previously placed grains. If the increase in the number of neighbors is beneficial to the majority of the previous grains, the first criterion is passed. Due to space limitations, the remainder of the placement criteria cannot be discussed here, but can be found in Reference 30. This process is carried out until every grain is successfully placed. Upon placement of all the grains, the CGP fills any remaining empty space by assigning these voxels to existing grains using a coarsening routine.[30]

The third module, Seed Point Generator–Constrained Voronoi Tessellation Tool (SPG–CVTT), uses the voxelized volume generated by CGP and generates seed points for a voronoi tessellation. The SPG–CVTT uses the centroids of

the grains as seed points and creates additional seed points to constrain the voronoi cell boundaries to pass closely to the voxelized grain boundaries. If only the centroids of the grains are used as seed points, the volume of larger grains is transferred to smaller grain, and the use of additional points (generally inside of larger grains) alleviates this problem. The frequency and location of additional seed points is outlined in detail in Reference 30.

After generation of the seed points, SPG–CVTT tessellates the structure and identifies the voronoi cells belonging to each grain. Note that after tessellation, every grain is comprised of a number of voronoi cells, and the larger grains generally have many more cells. The SPG–CVTT module deletes the "internal" faces that are shared between cells belonging to the same grain. This is because the internal faces have no physical meaning and only the external facets are needed. Visually the resulting structure appears to be similar to the experimental volume, as shown in Figure 5. Figure 5a is the statistically equivalent voxel volume from CGP and Figure 5b is the smoothed volume after Voronoi tessellation by SPG–CVTT.

The fourth module, Orientation Assignment Routine (OAR), is responsible for the assignment of orientations

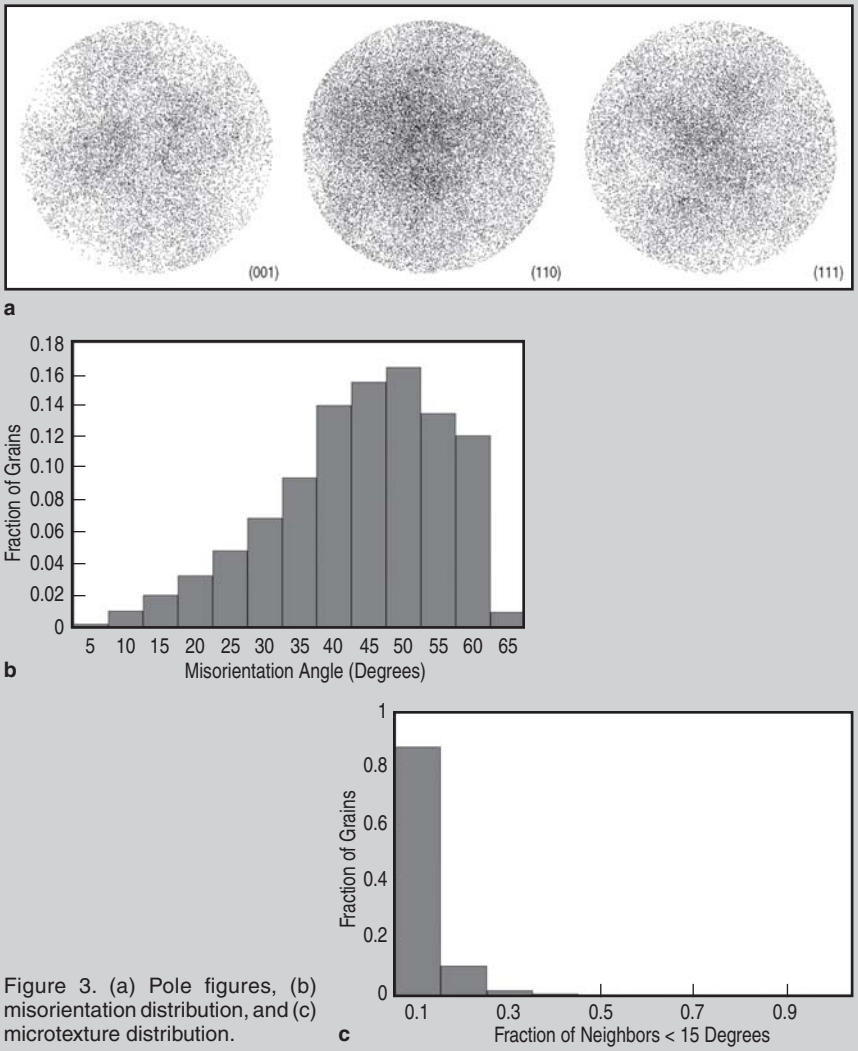

Figure 3. (a) Pole figures, (b) misorientation distribution, and (c) microtexture distribution.

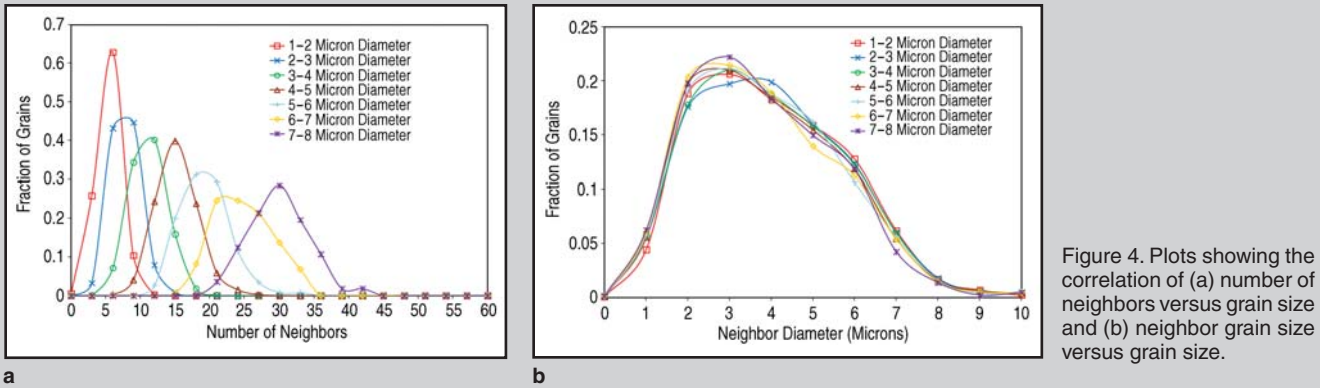

Figure 4. Plots showing the correlation of (a) number of neighbors versus grain size and (b) neighbor grain size versus grain size.

Figure 5. Volumes generated by (a) Constrained Grain Packer and (b) Seed Point Generator-Constrained Voronoi Tessellation Tool. The volume in (a) is voxelized and contains approximately 10 million elements. The volume in (b) has been smoothed and contains approximately 1.5 million elements. Compare with the experimental volume seen in Figure 1.

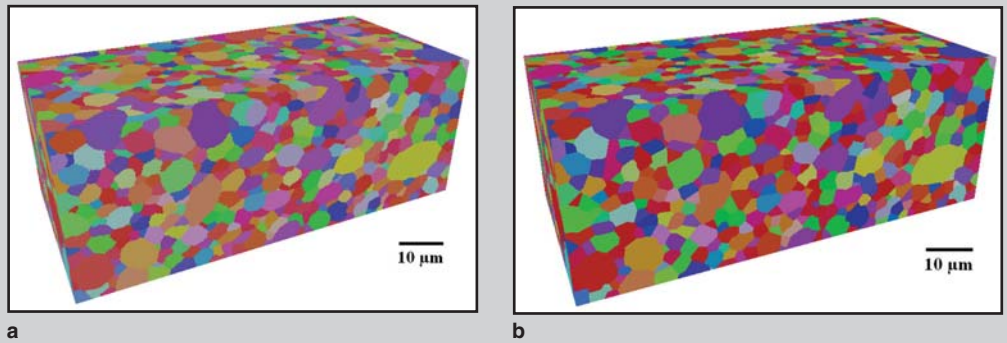

to the grains. Orientation Assignment Routine uses the ODF and MoDF from the experimental data to assign orientations to the smoothed grains. The orientations are generated by sampling the ODF and are initially assigned randomly as described in Reference 29. The MoDF of the synthetic structure is then calculated and compared to the experimental MoDF. The bins of the synthetic structure MODF that deviate most significantly from the experimental MoDF are identified, and grains contributing most to those bins are iteratively shuffled until the MoDF matches the experimental maps (this process can be thought of as a biased Monte Carlo method). The details of the orientation shuffling can be found in Reference 27. Additionally, the MTF is calculated after the MoDF is matched. A second biased Monte Carlo routine is employed to match the local microtexture.[27]

In addition to the visual agreement seen in Figure 5, it is desirable to compare the statistical distributions of the synthetic and experimental structures. Figure 6a–c shows a representative parameter from each of the characterization fronts (morphology, crystallography, and correlations). The distributions show good agreement between the two structures, further confirming the similarity of the two structures.

CONCLUSION

As a whole, this study is a first attempt to create a fully automated process that will collect 3-D microstructural information via serial sectioning, provide quantitative measurements of property-controlling microstructural features, and generate realistic statistically equivalent structures for modeling.

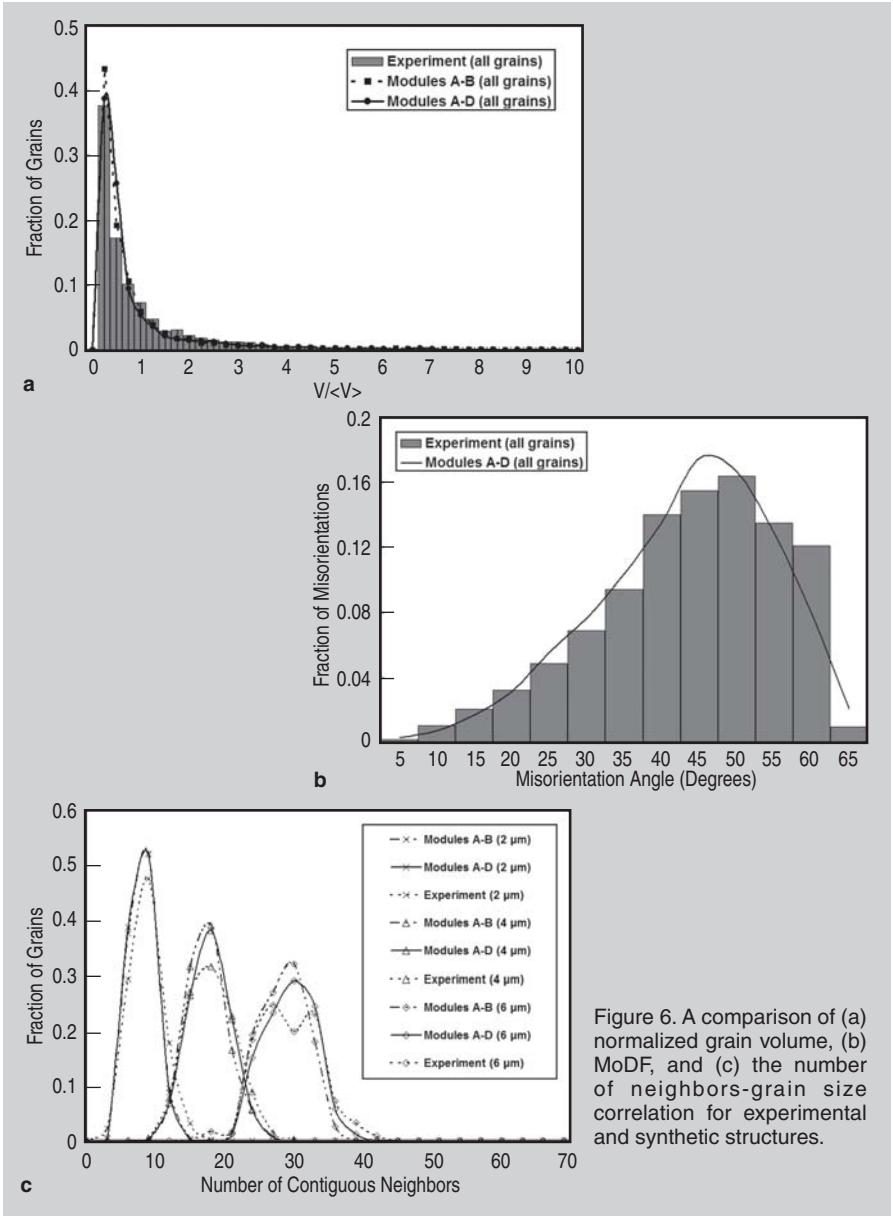

Figure 6. A comparison of (a) normalized grain volume, (b) MoDF, and (c) the number of neighbors-grain size correlation for experimental and synthetic structures.

References

1. M.D. Uchic, *JOM*, 58 (12) (2006), p. 24.
2. G. Spanos, *Scripta Mater.*, 55 (2006), pp. 3–5.
3. D.M. Dimiduk et al., *Numiform 8 Proceedings* (College Park, MD: AIP Publishers, 2004), pp. 1705–1710.
4. F.N. Rhines, K.R. Craig, and D.A. Rousse, *Metall. Trans. A*, 7A (1976), pp. 1729–1734.
5. N.R. Barton and P.R. Dawson, *Mod. and Sim. in Mater. Sci. and Eng.*, 9 (2001), pp. 433–463.
6. M. Coster et al., *Image Anal. Stereol.*, 24 (2005), pp. 105–116.
7. F. Ballani, D.J. Daley, and D. Stoyan, *Comp. Mater. Sci.,* 35 (2006), pp. 399–407.
8. O. Forsman, *Jern-Kontorets Ann.*, 102 (1918), pp. 1–30.
9. R.H. Hopkins and R.W. Kraft, *Trans. AIME,* 233 (1965), pp. 1526–1532.
10. E.B. Hawbolt and L.C. Brown, *Trans. AIME,* 239 (1967), pp. 1916–1924.
11. P.M. Ziolkowski, *The Three Dimensional Shapes of Grain Boundary Precipitates in a/b Brass* (Houghton, MI**:** Michigan Technological University, 1985).
12. R.T. DeHoff, *J. Microscopy,* 131 (1983), pp. 259–263.
13. K.M. Dobrich, C. Rau, and C.E. Krill, *Metall. Trans. A,* 35A (2004), pp. 1953–1961.
14. E.M. Lauridsen et al., *Scripta Materialia,* 55 (2006), pp. 51–56.
15. B.C. Larson et al., *Mater. Res. Soc. Symp. Proc.,* 590 (2000), pp. 247–252.
16. F.C. Hull, *Mater. Sci. Technol.,* 4 (1988), pp. 778–785.
17. D. Isheim et al., *Scripta Materialia,* 55 (2006), pp. 35–40.
18. M.D. Uchic et al., *Scripta Materialia,* 55 (2006), pp. 23–28.
19. M.A. Groeber et al., *Materials Characterization,* 57 (2006), pp. 259–273.
20. N. Zaafarani et al., *Acta Materialia,* 54 (2006), pp. 1863–1876.
21. R. Williams et al., *Proceedings Microscopy & Microanalysis*, 10 (2004), pp. 1178–1179.
22. J. Spowart, *Scripta Materialia,* 55 (2006), pp. 5–10.
23. Y. Bhandari, M. Groeber, and S. Ghosh, *CAD*, in review.
24. Y. Bhandari et al., *Comp. Mater. Sci.*, accepted for publication.
25. M. Groeber et al., *Acta Mater.*, in review.
26. M. Li et al., *Mater. Sci. and Eng. A*, A265 (1999), pp. 153–173.
27. D. Deka et al., *Metall. Trans. A,* 37A (2006), pp. 1371–1388.
28. D.M. Saylor et al., *Metall. Trans. A*, 35A (2004), pp. 1969–1979.
29. C.L. Xie, S. Ghosh, and M. Groeber, *J. Eng. Mater. Tech.*, 126 (2004), pp. 339–352.
30. M. Groeber et al., *Acta Mater.*, in review.

Michael Groeber is with Ohio State University, Department of Materials Science and Engineering, 477 College Rd., Columbus, OH 43210 USA; Somnath Ghosh is with Ohio State University, Department of Mechanical Engineering; and Michael D. Uchic and Dennis M. Dimiduk are with the Air Force Research Laboratory, Materials & Manufacturing Directorate, Wright-Patterson AFB, Ohio. Mr. Groeber can be reached at (614) 203-1403; e-mail groeber.9@osu.edu.